Effect of Contact Time and Force on Monocyte Adhesion to Vascular Endothelium

Kristina D. Rinker, Vikas Prabhakar, and George A. Truskey
Department of Biomedical Engineering, Duke University, Durham, North Carolina 27708 USA

ABSTRACT In this study we examined whether monocytic cell attachment to vascular endothelium was affected by elevating shear stress at a constant shear rate. Contact time, which is inversely related to the shear rate, was fixed and viscosity elevated with dextran to increase the shear stress (and hence the net force on the cell) independently of shear rate. At a fixed contact time, tethering frequencies increased, rolling velocities decreased, and median arrest durations increased with increasing shear stress. Rolling and short arrests ($<$0.2 s) were well fit by a single exponential consistent with adhesion via the formation of a single additional bond. The cell dissociation constant, k_{off}, increased when the shear stress was elevated at constant shear rate. Firmly adherent cells arresting for at least 0.2 s were well fit by a stochastic model involving dissociation from multiple bonds. Therefore, at a fixed contact time and increasing shear stress, bonds formed more frequently for rolling cells resulting in more short arrests, and more bonds formed for firmly arresting cells resulting in longer arrest durations. Possible mechanisms for this increased adhesion include greater monocyte deformation and/or more frequent penetration of microvilli through steric and charge barriers.

INTRODUCTION

Monocyte adhesion to vascular endothelium, an important initial event in atherosclerosis, is mediated via several receptors (Watanabe and Fan, 1998). Endothelium activated with the cytokine tumor necrosis factor-α (TNF-α) express E-selectin, intracellular adhesion molecule-1 (ICAM-1), and vascular cell adhesion molecule-1 (VCAM-1). Initial attachment and rolling of monocytes results from binding of E-selectin to its sialyl Lewis carbohydrate ligand. ICAM-1 and VCAM-1 binding to integrins on monocytes produces rolling and firm adhesion (Beekhuizen and van Furth, 1993; Kukreti et al., 1997; Reinhardt and Kubes, 1998; Takahashi et al., 1994). Monocytes contact the endothelium at a rate dependent upon the fluid dynamics and adhere through receptor-ligand bonds with a probability that varies with the flow rate. A recent theoretical study found that convective transport can significantly influence the intrinsic rate constant for adhesion (Chang and Hammer, 1999). Corresponding experimental measurements for cell adhesion to surface-immobilized antigen (Swift et al., 1998) showed that the rate constant for attachment varied in a manner not predicted by a model that considers attachment to be controlled only by contact time.

Adherent cells may firmly arrest or roll across the endothelium. Cell rolling is typically an erratic phenomenon that involves a balance between bond formation and breakage. The random nature of leukocyte rolling is due to the non-uniform distribution of microvilli and adhesion molecules (Bruehl et al., 1996; Hammer and Apte, 1992; von Andrian et al., 1995). Monocytes have microvilli that vary in length to a greater extent than lymphocytes and 72 $\pm$ 10% of cell surface L-selectin is located on microvilli (Bruehl et al., 1996). Clustering of adhesion receptors on microvilli may be more important at shear stresses above 3 dyn/cm^2, where microvilli are the predominant contact points and more bonds are needed to capture the leukocyte (Hammer and Apte, 1992; von Andrian et al., 1995). The stochastic nature of cell rolling has been incorporated in some models to predict the fluctuations in velocity (Hammer and Apte, 1992; Zhao et al., 1995; Zhu, 2000).

By analysis of cell detachment kinetics alone, cell adhesion would appear less likely in high-shear environments. However, neutrophils roll slower and more steadily on ligand surfaces at higher shear stresses due to the formation of an increased number of bonds (Chen and Springer, 1999). This and other in vitro studies have varied the flow rate (and thus both the shear stress and rate) to investigate changes in adhesion and rolling (e.g., Lawrence et al., 1997). The role of applied force has been clearly demonstrated in the detachment process (e.g., Alon et al., 1995, 1997; Smith et al., 1999). Less is known about the relative contribution of contact time and applied force on the attachment process. Neutrophil aggregation studies that mimic adhesion to vascular endothelium have been performed in which shear stress and shear rate were independently varied using a cone and plate viscometer and the viscosity elevated with Ficoll (Taylor et al., 1996). Aggregation increased by ~40% with a doubling of viscosity (from 0.75 to 1.7 cP) at constant shear rates of either 100 or 200 s^{-1}. This behavior was reversed at shear rates above 800 s^{-1}, where aggregation decreased. Correspondingly, adhesion efficiency increased rapidly with shear stress to a maximum at 5–10 dyn/cm^2, then decreased more slowly. Adhesion was primarily me-

Received for publication 22 March 2000 and in final form 16 January 2001.

K. D. Rinker's current address: Department of Chemical Engineering, Colorado State University, Fort Collins, CO 80523.

Address reprint requests to Dr. Kristina Rinker, 100 Glover Bldg., Fort Collins, CO 80523-1370. Tel.: 970-491-4648; Fax: 970-491-7369; E-mail: rinker@engr.colostate.edu.

0006-3495/01/04/1722/11 $2.00

diated by L-selectin and β_2-integrins, which are also important in monocyte adhesion.

In this study, the influence of contact time and shear stress on the initial attachment of monocytes to activated endothelium in parallel-plate flow chambers was determined by separately adjusting the flow rate and viscosity. Flux-corrected tethering frequencies, cell arrests, and rolling velocities were determined. Data were analyzed in terms of kinetic models for single and multiple bonds. For a fixed shear rate, the increase in shear stress increased the probability of bond formation. This resulted in increased adhesion frequency and decreased the rolling velocity number of bonds formed, possibly due to more frequent penetration of steric and repulsive barriers.

MATERIALS AND METHODS

Endothelial cell culture

Human umbilical vein endothelial cells (HUVECs; Clonetics, Walkersville, MD) were maintained in endothelial growth medium (EGM; Clonetics) supplemented with a mixture from Clonetics containing human epidermal growth factor, hydrocortisone, gentamicin, amphotericin B, bovine brain extract, heparin, and fetal bovine serum (FBS). Cells were grown in ventilated T-25 tissue culture flasks (Corning, Corning, NY) coated with 0.1% porcine gelatin (Sigma Chemical Co., St. Louis, MO) in M199 (Sigma). Flasks containing confluent monolayers of HUVECs were split 1:3 or 1:4 using trypsin/EDTA and trypsin neutralizing solution (Clonetics). For flow assays, cells were plated on gelatin-coated glass microscope slides. Slides plated with HUVECs were maintained at 37°C and typically reached confluency in 4–7 days. HUVECs of passage five or less were used in flow adhesion studies. On the day of the experiment, HUVEC monolayers were activated with 100 U/ml TNF-α (Sigma) for 4 h at 37°C.

Monocytic cell line

Mono Mac 6 cells (Erl et al., 1995) were maintained in RPMI-1640 medium (Sigma) supplemented with oxaloacetate, pyruvate, and insulin (OPI media supplement; Sigma), 10 ml/L minimal essential medium nonessential amino acids (Gibco/Life Technologies, Gaithersburg, MD), 10% heat-inactivated FBS (Sigma), 1% antibiotic/antimycotic solution (Sigma), and 2 mM L-glutamine (Sigma) in suspension. Cells were grown in tissue culture flasks and split every 2–3 days to maintain a cell concentration of 1.0×10^5 to 5.0×10^5 cells/ml. For flow assays, Mono Mac 6 cells were resuspended in media at 2.5×10^5 to 3.5×10^5 cells/ml. Mono Mac 6 cells were used in place of human monocytes due to the large number of cells required for the flow experiments and the decreased variability between experiments. Mono Mac 6 cells express many of the adhesion receptors found on human monocytes (Erl et al., 1995). Other properties affecting monocyte adhesion, such as cell deformation and receptor avidity, have not been evaluated for Mono Mac 6 cells to date and therefore may result in some difference compared with human monocytes.

Flow cytometry

Mono Mac 6 cells were incubated in the absence or presence of 5% dextran for 2 h at 37°C, then centrifuged at 500× *g* for 5 min. Cells were incubated with 5% mouse serum for 10 min to block Fc-specific sites and nonspecific binding, washed with PBS, and incubated with a 1:20 dilution of conjugated primary antibodies in PBS containing 2% bovine serum albumin and 0.1% sodium azide for 30 min at 4°C. The following primary antibodies were used: CD11b-FITC (clone 44, Sigma), CD18-FITC (clone 6.7, Pharmingen), CD11a-FITC (clone DF1524, Sigma), CD62L-FITC (clone FMC-46, Sigma), and CD49d-R-PE (clone 9F10, Pharmingen, San Diego, CA). CD11a and CD11b are α-integrin subunits that pair with the β-integrin, CD18, to form LFA-1 and MAC-1, receptors for ICAM-1 on the endothelial cell surface. CD49d is the α-chain for VLA-1, which binds to VCAM-1 on endothelial cells, whereas CD62L (L-selectin) binds to endothelial carbohydrate chains. IgG1-FITC, IgG1-R-PE, and IgG2bFITC (Sigma) were the isotype controls. Cells were washed and resuspended in PBS. For each sample the mean fluorescence intensity per cell and percent positive population were determined on a FACSCAN (Becton-Dickinson, Mountain View, CA) at the Duke University Comprehensive Cancer Center Flow Cytometry Facility.

Flow assays

Fixed- and variable-height flow chambers were used to establish laminar shear flow over a HUVEC monolayer. The variable-height flow chamber has an aluminum bottom plate separated from a Plexiglas top plate by a 500-μm-thick silastic gasket (Dow Corning, Midland, MI) with a removed rectangular section to form the flow channel. The Plexiglas top plate has a 2.22-cm-wide rectangular recess, which varies in depth from 500 μm at the inlet to 0 μm at the outlet. The resulting flow channel varies in height from ~1000 μm to 500 μm. The aluminum bottom plate has a rectangular hole with a groove to hold a glass microscope slide with HUVECs and permit viewing on an inverted microscope. Flow of RPMI-1640 media through the chamber was generated using a 60-cc syringe mounted on a syringe pump (Orion Research M362, Boston, MA). For a given volumetric flow rate Q, the wall shear rate $\dot{\gamma}$ (s^{-1}) is

$$\dot{\gamma} = \frac{6Q}{wh^2}, \tag{1}$$

where w is the width of the chamber and h is the total height. The wall shear stress τ_w (dyn/cm^2) is related to shear rate by viscosity, μ:

$$\tau_w = \mu\dot{\gamma} \tag{2}$$

Viscosity measurements

Viscosities of the media were determined using a cone-and-plate Brookfield viscometer (DV-III programmable rheometer, Brookfield Engineering Laboratories, Middleboro, MA) and data-gathering software (Rheocalc v1.0, Brookfield). Solutions of varying viscosity were prepared with 2×10^6 MW dextran (Sigma) in RPMI-1640 containing 10% FBS (Table 1). High-molecular-weight dextran was used to minimize the change in osmolarity of the medium (5% 2×10^6 MW dextran was determined to change the osmolarity of 10% FBS in RPMI-1640 by ~0.025 mosmol). Measurements were taken over a range of shear rates at 37°C. Pure RPMI-1640 media exhibited Newtonian behavior, and its viscosity was

TABLE 1 Viscosity of dextran solutions

Percent dextran in RPMI-1640	Average viscosity at 37°C (cP)
0	0.79 ± 0.01
1	1.40 ± 0.01
2	2.50 ± 0.01
3	4.30 ± 0.02
4	5.90 ± 0.01
5	7.30 ± 0.02

close to the value for water. The 5% dextran media exhibited slight deviations from Newtonian behavior.

Shear flow experiments

Confluent HUVEC monolayers on glass slides were activated for 4 h at 37°C with EGM media containing 100 U/ml TNF-α. Following incubation, the HUVEC monolayers were mounted in the flow chamber and placed on an inverted microscope (Nikon Diaphot-TMD) with a ×20 phase contrast objective. A heat lamp maintained the temperature at 37°C for the flow chamber outlet and 33°C for the inlet. Therefore, the medium viscosity varies 8% through the chamber. The HUVEC monolayer was perfused with media containing 0%, 3%, or 5% dextran at a shear rate of 10 s^{-1} for 15 min. Next, the HUVEC monolayer was perfused with 3×10^5 Mono Mac 6 cells/ml in media of each viscosity at shear rates of 20, 40, 80, and 120 s^{-1} for ~5 min at each shear rate. Experiments were performed in triplicate.

To assess the effect of dextran on adhesion, control experiments were performed as follows. A flow chamber containing a confluent layer of HUVECs was pre-infused with either 0% or 5% dextran for 5 min at 40 s^{-1}. Adhesion was measured for Mono Mac 6 cells resuspended in either 0% or 5% dextran at shear rates of 40, 80, and 120 s^{-1} Duplicate control experiments were performed.

Flow experiments were recorded on videotape using a video camera (MTI PA-70, Michigan City, IN) and video recorder (Panasonic AG-1980P, Secaucus, NJ) equipped with a time-date generator (VTG-33, FOR.A, Cypress, CA). The field of view was 640 μm long (direction of flow) by 480 μm. Camera gain and black level were set to maximize contrast between monocytes and background. Mono Mac 6 cells were tracked across the HUVEC monolayers with the use of a video recorder with jog-shuttle capability (Panasonic AG-1980P) and a computer-assisted system. Analysis was performed on a Macintosh computer using National Institutes of Health Image 1.62a. The hydrodynamic velocity of non-interacting cells is 14.108$\dot{\gamma}$ (Barber, 1997). Macro programs were written to determine cell arrest durations and rolling velocities.

Instantaneous cell velocities

The velocity of individual cells was tracked for the duration that the cell interacted with the endothelium on a frame-by-frame basis (30 frames/s). Pause durations were determined from the cell trajectories using a threshold of 15% of the hydrodynamic velocity. This threshold was chosen after tape analysis as the upper velocity limit of most of the rolling cells. Cells moving at a velocity above this threshold generally moved at a constant speed and did not appear to be interacting with the endothelium. This value is similar to the threshold of 30 μm/s above the lowest rolling velocity used by Chen and Springer (1999). Most slow rolling cells stayed below this threshold whereas non-interacting cells predominated above the threshold. Rolling pauses were defined according to Chen and Springer (1999) as the time the cells spent between the threshold velocity and an arrest or rise in velocity above the threshold. Short arrest durations included the time the cells arrested (from 0.033 to 0.2 s) during rolling. Both pause durations and short arrests were modeled as a first-order process assuming a single additional bond was formed with the slope of the natural logarithm of bound cells versus the time of pause or arrest being $-k_{off}$.

Tethering frequencies

The tethering frequency, f_t, was determined as the number of cells that adhered to the endothelium per unit time and area and includes rolling and firmly arrested cells. This frequency was normalized by cell flux to the surface, which is the product of the cell concentration adjacent to the surface, ψ, times the sedimentation velocity, V_s, (Munn et al., 1994):

$$V_s = \frac{2(\rho_c - \rho)gR^2}{9\mu}, \tag{3}$$

where ρ is the density of the fluid, ρ_c is the density of the cell (1.07 g/cm^3), g is gravitational acceleration, μ is viscosity, and R is the radius of the cell (6.5×10^{-4} cm). Sampling in the steady-state portion of the flow chamber, the dimensionless concentration is (Munn et al., 1994)

$$\frac{\psi}{c} = 1 + \frac{v_s x}{uh}, \tag{4}$$

where c is the concentration of cells in the bulk fluid, h is the depth of field (13×10^{-4} cm), x is the distance along the length of the slide at which adhesion is measured (3.81 cm), and u is the fluid velocity. Corrected tethering frequencies were determined by normalizing the dimensionless concentration against the value at the lowest shear stress and shear rate condition performed then multiplying by the experimentally determined tethering frequency.

Forces on adherent monocytes and tether formation

When a Mono Mac cell of radius R (6.5 μm (Erl et al., 1995)) forms one or more bonds with counter-receptors on the endothelium, fluid shear stresses exert a torque (T) and drag force (F_x) on the Mono Mac cell (Fig. 1). The net hydrodynamic force on the cell is balanced by a force (F_b) that stresses the microvillus of length L and the bonds.

Because the Reynolds number ($Re = 2\rho R^2\dot{\gamma}/\mu$, where $\dot{\gamma}$ is the shear rate, ρ is the fluid density, and μ is the fluid viscosity) is much less than one, inertial forces are negligible and the drag force and torque are given by (Goldman et al., 1967)

$$F_x = F_x^* 6\pi R^2 \tau \tag{5}$$

$$T = T_y^* 4\pi R^3 \tau, \tag{6}$$

where F_x^s* and T_y^2* are functions of the separation distance of the cell from the surface. For the case of a cell touching the surface, F_x^s* = 1.7005 and

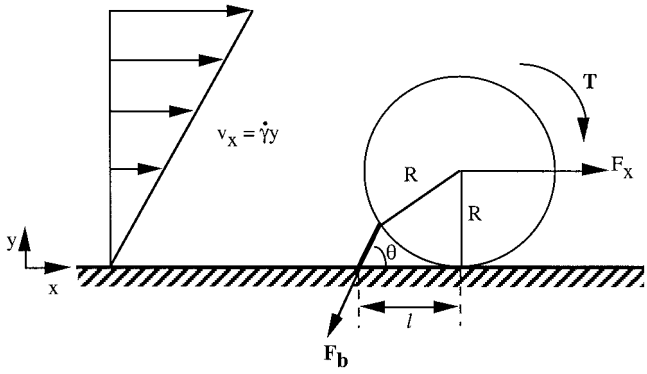

FIGURE 1 Model for fluid-induced forces acting on a monocyte rolling across an endothelial monolayer in laminar shear flow. Fluid flows at a velocity v_x and exerts a drag force F_x and torque T. The cell of radius R is tethered by one or more bonds on a microvillus of length L. The net hydrodynamic force on the cell is balanced by a force (F_b) that stresses the microvillus of length L and the bonds at the tip of the microvillus. The microvillus is at an angle θ relative to the surface. The lever arm is of length l.

$T_y^{2*} = 0.94399$ (Goldman et al., 1967). By calculating the x component of the force and performing a torque balance one obtains (Shao et al., 1998)

$$F_b \cos\theta = 32.054R^2\tau \tag{7}$$

$$F_b/\sin\theta = 43.916R^3\tau, \tag{8}$$

Where l is the lever arm and

$$\theta = \tan^{-1}\left(\frac{R}{l}\right) + \cos^{-1}\left(\frac{l^2 + L^2}{2L\sqrt{l^2 + R^2}}\right). \tag{9}$$

When the applied force on a microvillus exceeds a critical value of 45 pN, membrane tethers form (Shao and Hochmuth, 1998). Membrane tether formation has been observed in vitro under physiological flow conditions (Schmidtke and Diamond, 2000). After a tether forms, L and l increase and the net force on the bonds decline. Because the mean lifetime of bonds declines at higher forces (Alon et al., 1995), tether formation results in longer bond lifetimes.

For forces below the critical value, the microvillus behaves as an elastic material (Shao et al., 1998), and the force on the bonds is given by

$$F_b = k_1(L - L_o), \tag{10}$$

where L_o is the length of an unstressed microvillus, 0.35 μm (Shao et al., 1998). The spring constant for microvilli k_1 was assumed to be the same on Mono Mac 6 cells as it is for neutrophils, 43 pN/μm (Shao et al., 1998). Once the critical force F_o is exceeded, tethers form according to the following relation:

$$F_b = F_o + k_2\frac{dL}{dt}, \tag{11}$$

where $k_2 = 11$ pN s/μm (Shao et al., 1998).

Kinetics analysis of firm arrests

To determine the effect of tether extension on bond lifetime, we used a kinetic model for formation of a small number of bonds. Firm arrests were defined as occurring if a cell moved less than 3 μm for greater than 0.2 s. The kinetic analysis is based on the assumption that adhesion and rolling of monocytes on endothelium are mediated by a small number of bonds. This assumption is supported by a number of experimental and theoretical studies. Leukocyte arrest durations over purified ligands at low ligand densities is described by a first-order process suggestive of single bond formation (Alon et al., 1995). At higher densities, multiple bond formation appears to occur. A small number of bonds appears to be involved in leukocyte rolling over purified selectins (Chen and Springer, 1999), micropipette adhesion assays (Shao and Hochmuth, 1998; Chesla et al., 1998), and in neutrophil attachment to TNF-α-activated endothelium under low shear stresses (Kaplanski et al., 1993).

To model firm arrest durations, bond formation is assumed to be a stochastic process. The initial number of bonds formed is distributed among the population according to a Poisson distribution. The average number of bonds formed is $\langle n\rangle$. The probability ($P(n)$) of initially forming n bonds is

$$P(n) = \frac{\exp(-\langle n\rangle)\langle n\rangle^n}{n!}, \tag{12}$$

where $n = 0, 1, 2, 3, \ldots$.

After these n bonds form during an arrest event, the bonds can dissociate or new bonds can form. The probability of forming i bonds is (Kaplanski et al., 1993; Cozens-Roberts et al., 1990; Chesla et al., 1998)

$$\frac{dp_i}{dt} = (i+1)k_{off}^{i+1}p_i + k_{on}C_L(R - (i-1))p_{i-1} - ik_{off}^{i+1}p_i - k_{on}C_L(R - i)p_i, \tag{13}$$

where C_L is the surface concentration of ligand molecules, R is the number of receptor molecules in the contact region, k_{on} is the association rate constant, and k_{off}^i is the dissociation rate constant for the ith bond. Assuming that all bonds are stressed equally, k_{off}^i equals

$$k_{off}^i = k_{off}^o \exp\left(\frac{\sigma F}{ikT}\right), \tag{14}$$

where k_{off}^o is the unstressed dissociation constant, σ is the characteristic length of stretching, F is the force on the cell, i is the number of bonds, k is Boltzmann's constant, and T is the absolute temperature. The total probability of forming bonds is $p = \Sigma_{i=1}^{\infty} p_i$.

To simplify the analysis, the number of receptor molecules is assumed to be much greater than the number of bonds formed so that the receptor number is approximately constant. C_L is also assumed to be large relative to the number of bonds formed. The probability of forming new bonds is also assumed to be very low during the attachment time, and Eq. 13 simplifies to

$$\frac{dp_i}{dt} = (i+1)k_{off}p_{i+1} - ik_{off}p_i \quad i = 1, 2, \ldots, n. \tag{15}$$

At time 0, $p_n = 1$ and $p_i = 0$ for i ranging from 1 to $n - 1$. Solving Eq. 15 for $i = 1$ to n and summing yields the total probability distribution of bonds when a cell adheres with n bonds formed initially:

$$p(n, t) = \sum_{i=1}^{n} \exp(-ik_{off}^i t) \prod_{\substack{j=1 \\ j\neq i}}^{n} \frac{jk_{off}^j}{jk_{off}^j - ik_{off}^i} \tag{16}$$

For a population of cells adhering initially with a probability distribution of forming n bonds given by Eq. 12, the probability of adhesion for the population of attached cells as a function of time, $P_{adh}(t)$, is

$$P_{adh}(t) = \sum_{n=1}^{\infty}\left(\frac{\exp(-\langle n\rangle)\langle n\rangle^n p(n)}{n!(1 - \exp(-\langle n\rangle))}\right), \tag{17}$$

where the term $1 - \exp(-\langle n\rangle)$ in the denominator of the Poisson distribution accounts for the fact that only adhesive events are measured.

When the applied force on a bond exceeds a critical value of 45 pN (Shao and Hochmuth, 1998) membrane tethers may form. After a tether forms, the force per bond declines with time and bond lifetimes are longer than they would be if no tether formed.

For computational purposes, the numerical solutions of force versus time generated by the model of Shao and Hochmuth (1998) were fit to the following function $F = at^b$. All fits exhibited values of r^2 greater than 0.90. Inclusion of a time-dependent force requires a numerical solution of Eqs. 15 and 16. Solutions were obtained using a Runge Kutta method on Matlab (The Mathworks, Natick, MA). Because force is weakly dependent upon time (b ranged from -0.14 to -0.19), we have found, however, that the analytical solution (Eq. 16) can be used with $F = at^b$. A systematic comparison shows that for lower shear stresses there is excellent agreement between the exact numerical result and the use of a time-dependent force in Eq. 16. At higher shear stresses and higher numbers of bonds per cell the approximate solution overestimates the approximate numerical solution by ~15%. Because of the computational advantages in nonlinear regression of

the model to data (Bates and Watts, 1988), the approximate solution was used.

Statistical analysis

All results are reported as the mean standard error unless otherwise stated. Differences among mean arrest durations were determined using a two-way ANOVA and Duncan test with Statistica for Macintosh software (Graphpad).

RESULTS

Dextran does not affect monocyte adhesion molecule surface expression

Flow cytometry for CD11a, CD11b, CD18, CD49d, and CD62L was performed on Mono Mac 6 cells incubated in the absence and presence of 5% dextran. Similar mean fluorescence intensities and percent positive antibody-labeled cells were found for the major adhesion molecules of Mono Mac 6 involved in endothelial cell adhesion. Cells incubated with dextran were elevated compared with the control by 1% for CD49d and CD11a, 2% for CD62L, 7.5% for CD11b, and 11.5% for CD18. These values are within experimental error, suggesting that number of adhesion receptors per cell is the same for control Mono Mac 6 cells and cells exposed to dextran for up to 2 h.

Effect of force at a fixed contact time on monocyte rolling

When both shear stress and shear rate increased, the average monocyte rolling velocity increased with flow rate. In contrast, when the effect of shear stress was isolated by increasing the viscosity at a constant shear rate, rolling velocities decreased with increasing shear stress up to 9 dyn/cm^2 (Fig. 2).

To assess whether dextran interacted with endothelium and affected attachment and rolling, rolling velocities were determined on HUVECs pre-infused with either 0% (0.8 cP) or 5% (7.3 cP) dextran (data not shown). After pre-infusion, Mono Mac 6 cells were infused in medium at either 0.8 or 7.3 cP. Pre-infusion led to small changes in rolling velocities, but the differences were not significant. Thus, the decrease in rolling velocities with elevated shear stress at the same shear rate is due to the elevation in force and not to artifacts arising from the use of dextran. Although 40,000 MW dextran increases the steric barriers and/or electrostatic shielding of endothelium, which may lead to decreased leukocyte adhesion (Baldwin et al., 1991), our results do not indicate that 2×10^6 MW dextran blocks adhesion.

Instantaneous velocities

To investigate the dynamics of rolling, instantaneous velocities were obtained for all interacting cells infused in 0.8-cP and 7.3-cP media. For each cell, the velocity was determined on a frame-by-frame basis from a video captured at 30 frames/s. Cells rolling on HUVECs in 0.8-cP media have a larger range of velocities than cells in 7.3-cP media (Figs. 3 and 4). At a shear rate of 40 s^{-1}, cell velocities deviate from the mean to a greater extent for cells in 0.8-cP media (shear stress 0.32 dyn/cm^2) than in 7.3-cP media (shear stress 2.92 dyn/cm^2). However, there are more arrests per cell at the higher shear stress (7.5 arrests/cell) than at the lower shear stress (4.7 arrests/cell).

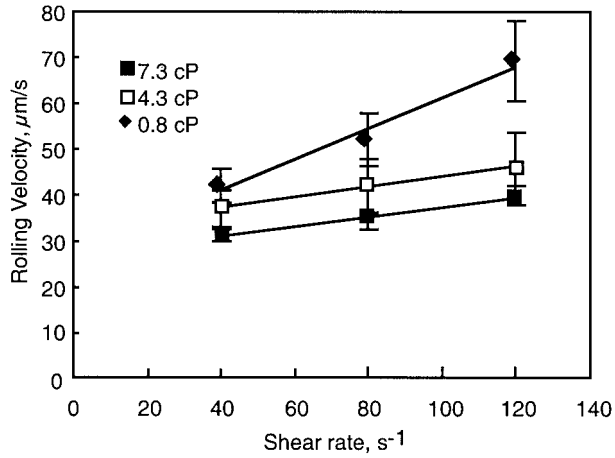

FIGURE 2 Effect of shear stress at constant shear rate on monocyte rolling velocities. Mono Mac 6 cells were perfused in RPMI-1640 media containing FBS over a confluent monolayer of HUVECs on a glass slide. Rolling velocity was determined as described in Materials and Methods. Fewer events occurred at the higher shear rates; however, at least 15 events were analyzed at the highest shear rate, 120 s^{-1}, for each experiment. Velocities from three experiments were averaged. Error bars represent the standard deviation from these experiments.

Analysis of step distances, which are the distances traveled by the cell between frames, further illustrates the stability of rolling. Long step distances represent tumbling events in which the cell is initially tethered, breaks free and travels for a distance with no adhesive interactions, and then tethers again (Chen and Springer, 1999). The cumulative distribution of step distances at a shear rate of 40 s^{-1} shows that cells had a shorter median step distance for the high-shear-stress case, therefore more steady rolling (Fig. 3 *C*). These shorter step distances at the higher shear stress suggest more efficient bond formation. The higher percentage of longer step distances for the low-shear-stress case illustrates the presence of more tumbling events and thereby more erratic rolling.

This effect is more exaggerated at a shear rate of 80 s^{-1}, in which cells in low-viscosity medium have tumbling events that reach much higher velocities than found for cells in higher viscosity medium (Fig. 4). As seen at 40 s^{-1}, the presence of more tumbling events in the low-viscosity medium is shown by a higher fraction of longer step distances (Fig. 4 *C*). This further illustrates that by increasing the

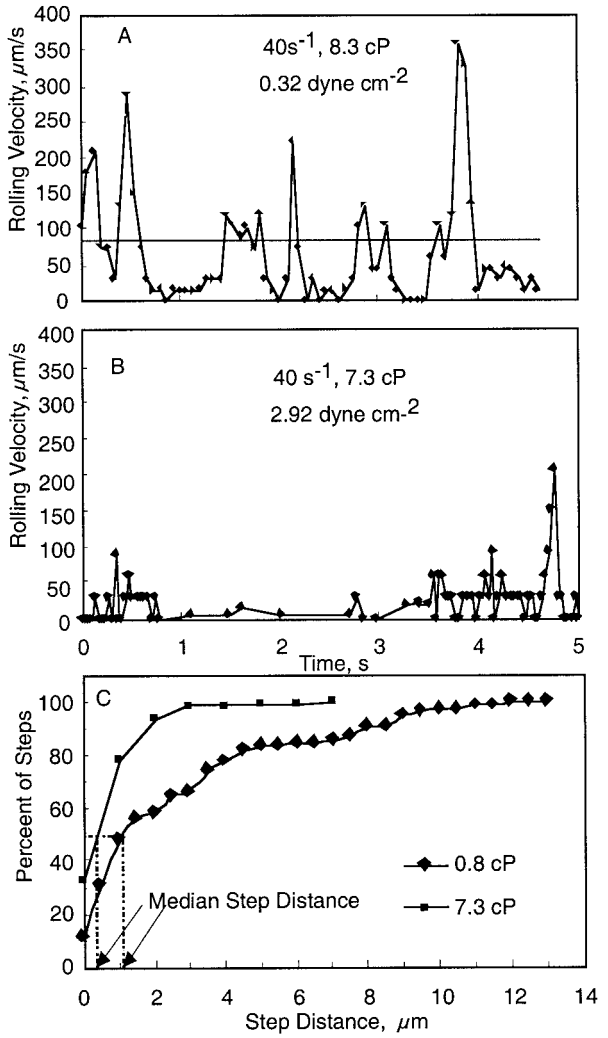

FIGURE 3 Instantaneous velocities for representative Mono Mac 6 cells rolling over the HUVEC monolayer in 0 (*A*) and 5% (*B*) dextran solutions at 40 s^{-1}. The horizontal line represents the threshold velocity of 85 μm/s. (*C*) Cumulative distribution of step distances between frames for the low- and high-viscosity cases in *A* and *B*. The distribution of steps for both cells shows a broader distribution and therefore more tumbling events at the lower-viscosity condition.

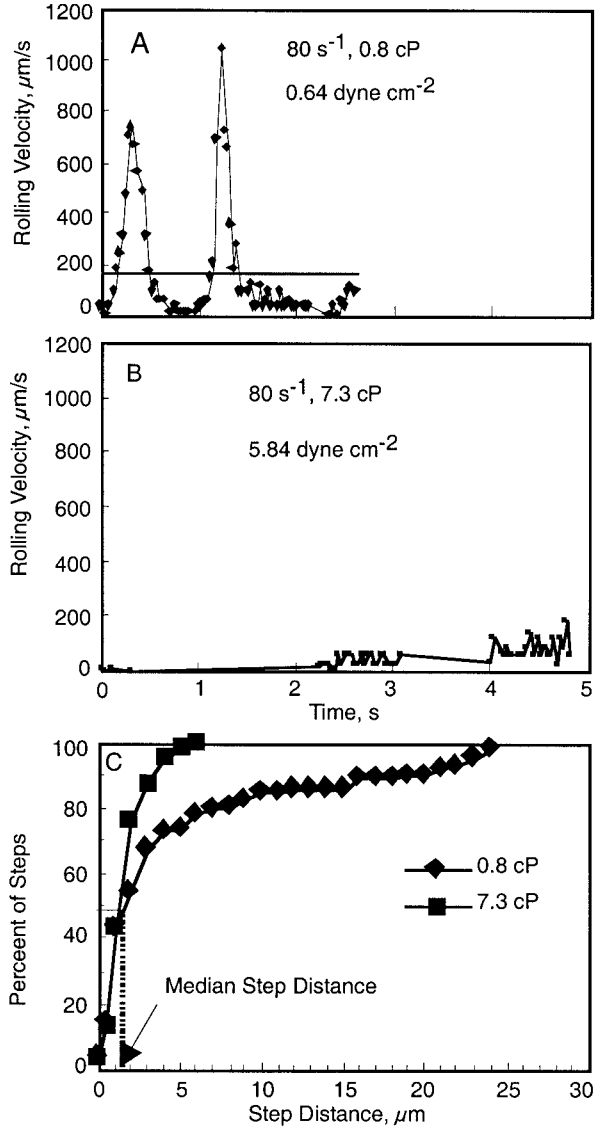

FIGURE 4 Instantaneous velocities (*A* and *B*) and median step distances (*C*) for a representative Mono Mac 6 cells rolling over the HUVEC monolayer in 0 (*A*) and 5% (*B*) dextran solutions at 80 s^{-1}. The horizontal line represents a threshold of 170 μm/s. The difference in median step distances at 80 s^{-1} (*C*) is smaller than found at 40 s^{-1} (Fig. 3 *C*).

force and maintaining a constant contact time, cells interacting with the endothelium have more constant velocity profiles and fewer tumbling events.

Kinetic models were used to analyze rolling below the threshold velocity and short-term arrest less than 0.2 s for cells infused at shear rates of 40 s^{-1} and 80 s^{-1}. At 0.8 cP, 16 cells were analyzed resulting in 117 pauses, and 11 cells had 52 arrests. At 7.3 cP, 67 pauses from 10 cells and 45 arrests from 6 cells were analyzed. Arrest (Fig. 5 *A*) and pause (Fig. 5, *B* and *C*) durations were fit well by a single-exponential model representing dissociation from a single bond. The dissociation rate constant k_{off} was greater for cells subjected to higher forces, as reported by others (Alon et al., 1997; Smith et al., 1999). The dissociation constant was larger for the short arrest process than the rolling pauses. Rolling cells must be forming bonds with the cell surface receptors. For a fixed contact time, formation of a single additional bond produces rolling pauses and short arrests. The difference in k_{off} determined from rolling pauses and short arrests may be due to the involvement of different receptors.

Tethering frequencies as a function of contact time and shear stress

The tethering frequency, the number of adhesive events (rolling or arrest) per unit time and area, was significantly

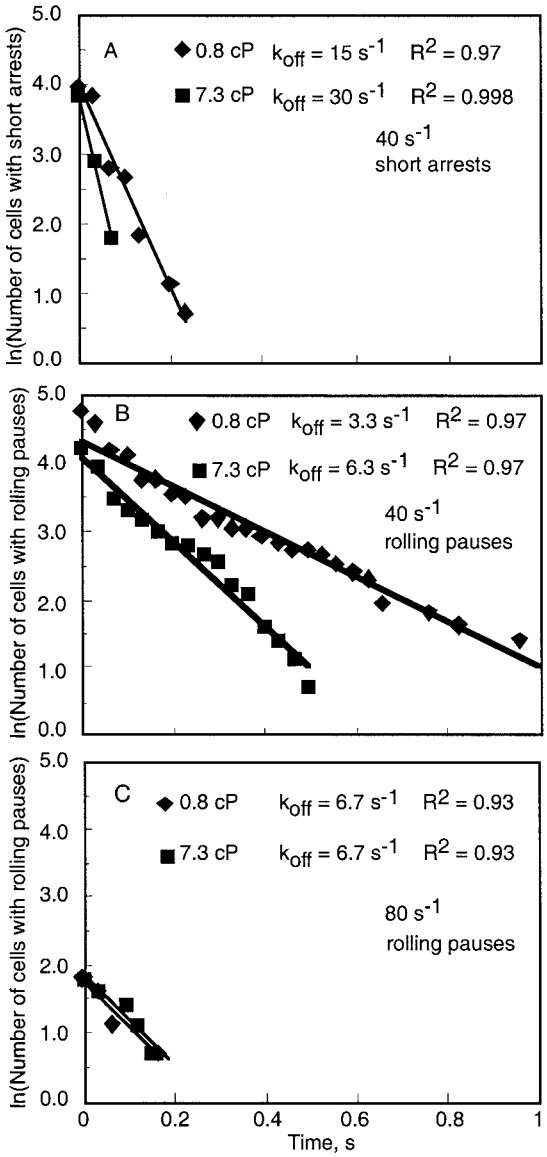

FIGURE 5 Increases in shear stress at a constant shear rate of 40 s^{-1} lead to an increase in the bond dissociation constant k_{off}. The data fit the model for single bond formation well. k_{off} was determined from instantaneous velocity profiles using short arrest durations (*A*) and pause durations (*B*), which excluded arrests and velocities above 15% of the hydrodynamic velocity. Cell dissociation constants, k_{off}, for pause durations at 80 s^{-1} (*C*) do not vary with shear stress as found for 40 s^{-1} (*B*).

affected by shear rate and shear stress (Fig. 6). All frequencies were corrected for the decrease in cell flux with increasing shear rate and viscosity and normalized against the lowest viscosity case (0.8 cP). At a fixed medium viscosity, the normalized tethering frequency decreased with increasing flow rate by an average of 4.9 ± 0.3-fold from 40 to 120 s^{-1}. When shear rate was held constant and shear stress varied, normalized tethering frequencies increased an average of 11.0 ± 2.3-fold as the viscosity increased from 0.8 to 7.3 cP. The tethering frequency was reduced when HUVECs

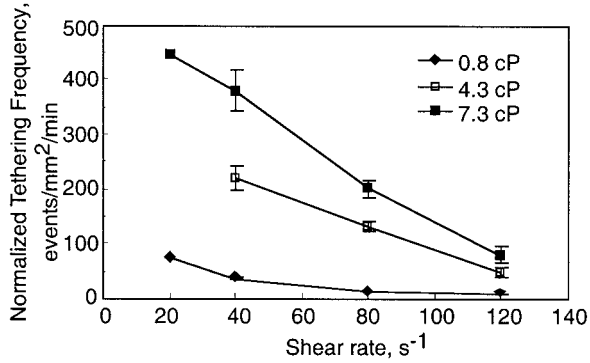

FIGURE 6 Effect of shear stress on tethering frequencies at fixed shear rates. When the shear rate is fixed, increasing the shear stress leads to increased tethering frequencies.

were incubated with antibodies to ICAM-1 or E-selectin before infusion of Mono Mac 6 cells. When the shear rate was fixed, the blocking antibodies had a greater effect upon tethering at higher shear stresses than at lower shear stresses.

Effect of force at a fixed contact time on monocyte arrests

Median arrest durations, determined for cells that arrested without rolling for at least 0.2 s, were affected by the applied force of the fluid. Median arrest durations decreased with increasing shear rate. For a fixed contact time, however, monocytes that adhered to endothelium at higher shear stresses arrested for longer times (Table 2). Analysis of variance of the arrest durations indicated that this effect of shear stress and contact time was significant. At shear rates of 40 s^{-1} and 80 s^{-1}, the arrest duration was dependent on medium viscosity and shear rate. At 120 s^{-1}, the increase in arrest duration with shear stress was not significant.

The effect of pre-infusion of 5% dextran on median arrest durations was also evaluated to assess whether dextran directly affected endothelial cell adhesive properties. Pre-

TABLE 2 Median arrest durations on TNF-α-activated HUVECs for Mono Mac 6 cells suspended in medium of increasing viscosity

Suspension viscosity (cP)	Median arrest duration (s) at constant shear rate		
	40 s^{-1}	80 s^{-1}	120 s^{-1}
0.8	1.31 ± 0.13	0.89 ± 0.03	0.23 ± 0.03
4.3	1.51 ± 0.17	1.14 ± 0.13*	0.28 ± 0.06
7.3	1.83 ± 0.12†	1.22 ± 0.09§	0.38 ± 0.01

Viscosity was elevated using 2 million molecular weight dextran. All arrest durations were significant with respect to shear rate to a maximum p = 0.02.
*p = 0.08.
†Effect of shear stress at constant shear rate significant to 0.01 compared with 40 s^{-1}.
‡$p < 0.05$ compared with 40 s^{-1} at constant shear rate.

infusion at a constant shear rate increased the median arrest duration of cells in 0% dextran by 4.9% and 6.4% and in 5% dextran by 3.6% and 6.4% at shear rates of 40 s^{-1} and 80 s^{-1}, respectively. In contrast, the difference in arrest durations for infusion of monocytes in 0% or 5% dextran ranged from 20.6% to 26.5%. Except for a shear rate of 120 s^{-1}, this difference is much less than the difference due to the change in monocyte adhesion with shear stress. The small difference between the pre-infusion effect for cells infused in 0% and 5% dextran implies that only a small percentage of the pre-infusion effect is due to a direct interaction between dextran and the endothelium.

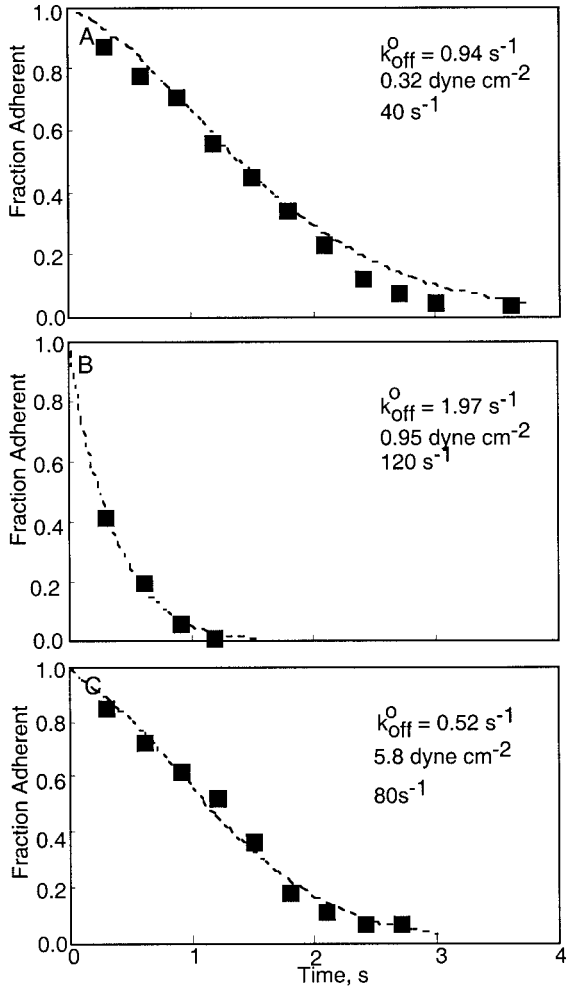

FIGURE 7 The fraction of cells remaining adherent with time for a shear rate of 40 s^{-1} and shear stress of 0.32 dyn/cm^2 (*A*), a shear rate of 120 s^{-1} and a shear stress of 0.95 dyn/cm^2 (*B*), and a shear rate of 80 s^{-1} with a shear stress of 5.8 dyn/cm^2 (*C*). Shear stress was elevated using 3% and 5% dextran. The data were fit to the Bell model, $k_{off} = k^o_{off}\exp(\sigma F/kTi)$ where σ is the distance over which the bond is stretched, k is the Boltzmann's constant, and i is the number of bonds formed (Bell, 1978). The force was calculated using $F = at^b$ according to Shao and Hochmuth (1998) assuming two stressed tethers per cell. R^2 values were equal to or greater than 0.90.

The increase in median arrest durations at higher shear stress appears to be due to formation of more bonds during the initial contact (Fig. 7). The convex shape at lower shear stresses is not consistent with a first-order process arising from breakage of a single bond. Several peaks are evident in many of the arrest duration histograms, indicating multiple bonds may form and break (data not shown). The fraction of adherent cells as a function of time was fit well by a model that assumed multiple bond formation and no bond reformation (Eqs. 15 and 16.)

For a fixed contact time, the resulting average bond densities increased with increasing shear stress (Fig. 8 *A*). Except for the 0.8-cP case, k^o_{off} appears to be independent of shear stress (Fig. 8 *B*). Regression of the data failed to detect a significant trend with shear stress ($r^2 = 0.41$, $p = 0.09$). From this kinetic analysis we conclude that the increase in median arrest durations at higher shear stress appears to be due to the formation of more bonds during the initial contact. These results do not, however, exclude the possibility that different receptors may be involved at shear stresses below 1 dyn/cm^2.

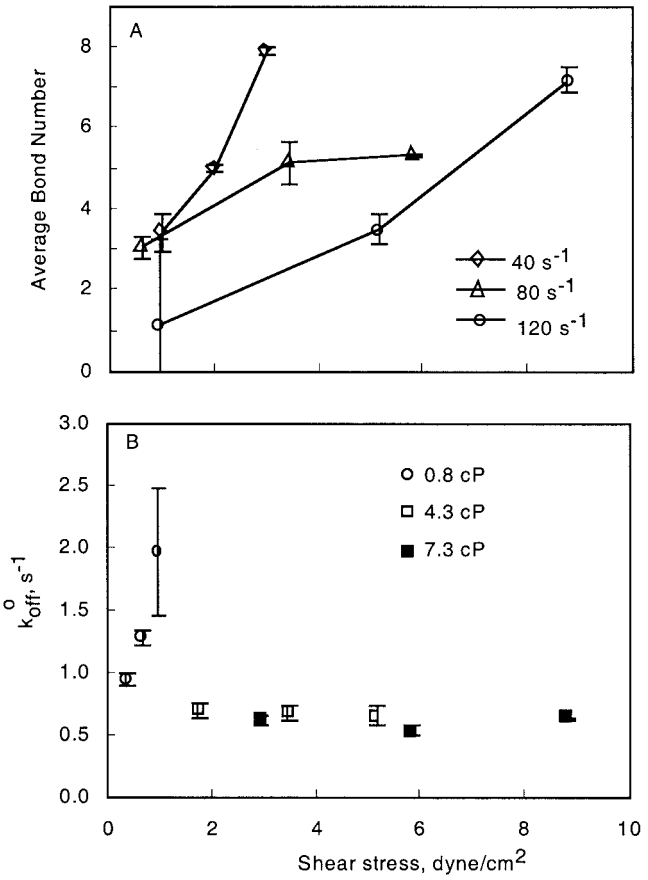

FIGURE 8 The effect of shear stress and shear rate on the average number of bonds formed, N (*A*), and the cell dissociation constant, k_{off} (*B*), as determined by a model for multiple bond formation in Fig. 7.

DISCUSSION

By separately varying fluid viscosity and flow rate, the contributions of contact time and force on the attachment and rolling process were isolated. For a fixed contact time, increasing the shear stress caused monocyte rolling velocities to decrease, whereas the adhesion frequency and median arrest duration increased. The kinetic analysis revealed that short arrests and rolling pauses were due to the formation of a single additional bond (Fig. 9). This is supported by the kinetic analysis of short arrests with a high-resolution system (Smith et al., 1999). At low shear stresses, cells form a single bond to initiate rolling but are less likely to form an additional bond immediately. Therefore, these cells roll quicker in a more erratic fashion as found by Chen and Springer (1999). At higher shear stresses, single bonds generally formed as each microvillus contacted the endothelium, thereby maintaining a slow and relatively steady rolling velocity. The median arrest duration for firmly adherent cells (arrested for at least 0.2 s) increased at higher shear stresses for the same contact time (Fig. 9). Kinetic modeling showed that arrests are due to the formation of multiple bonds. The data suggest that hydrodynamic forces affect both the formation of the initial bond leading to arrest as well as subsequent bond formation during rolling and arrest.

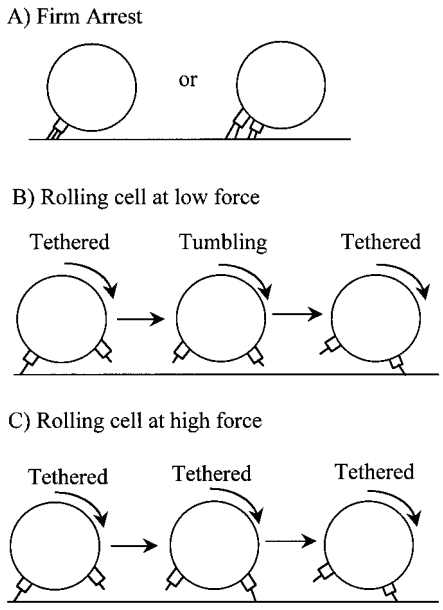

FIGURE 9 Monocyte adhesion mechanisms for low and high laminar shear stress. (*A*) Firm arrests occur when multiple bonds form. Cells that arrest firmly at high shear stresses form more bonds and arrest for longer periods of time than cells that arrest under low-shear-stress conditions. Rolling cells have more tumbling events in low shear stress (*B*) than in high shear stress (*C*) flow. At low shear forces, rolling cells do not form an adhesive bond with every cell rotation and therefore detach briefly before re-establishing a bond with the endothelium. Under high-shear-stress conditions, however, bonds are more likely to form with each cell rotation, resulting in slower, more regular translocation across the endothelium.

Although the tethering frequency decreased with increasing shear rate for a fixed contact time, the increase in the frequency of tethering events with applied shear stress (Fig. 6) is not consistent with a model of adhesion solely based upon convective transport and binding kinetics (Chang and Hammer, 1999). This difference between experiment and theory is not due to differences in the flux of cells passing the field of view, which was corrected to account for changes in flow rate and viscosity. At constant flux, the significant increase in adhesion implies a force dependence upon the binding interaction in addition to a contact-time dependence discussed by Chang and Hammer (1999).

By holding the contact time fixed as the force varied we found that once an initial adhesive interaction forms, increased forces at higher shear stresses increase the likelihood that subsequent bonds may form. This is illustrated in the rolling velocity data (Fig. 2) and instantaneous velocity profiles (Figs. 3 and 4) in which slower, more steady rolling occurred at higher shear stresses at the same shear rate. Chen and Springer (1999) observed a similar result for the kinetics of L-selectin bond formation when the shear stress and shear rate varied simultaneously. In these experiments, rolling appeared to be a two-step process; rapid bond formation and dissociation during a pause followed by a brief translation at the hydrodynamic velocity. Pauses occurred with regularity. Our results at 40 s^{-1} and 80 s^{-1} exhibit some of these features (Figs. 3 and 4), although the velocity fluctuations are not as regular as those observed by Chen and Springer (1999) due to the topography of the endothelium and nonuniform distribution of adhesion molecules. At higher shear stresses, velocity fluctuations were much lower (Figs. 3 *B* and 4 *B*), but the rolling velocity between arrests was much less than the hydrodynamic velocity. For this case, the higher forces may facilitate bond formation and reduce the cell velocity. At a fixed contact time, the rolling velocity at the lowest shear stresses involved pauses or short arrests followed by a rise to the hydrodynamic velocity.

Kinetic analysis of the lifetime of rolling and brief arrests indicated that a single bond could explain these events. For these conditions, rolling is likely due to formation of one bond that is sufficient to alter the cell velocity. At the higher shear stresses, the rolling velocity was much slower than the hydrodynamic velocity and pauses and arrests were more frequent. The distribution of pause and arrest times fit a first-order model as found by Smith et al. (1999). For such low rolling velocities, however, regular and multiple bond formation must be occurring before a pause or arrest; otherwise, the cell would detach. Because the values of k_{off} for arrest durations were much larger than the values for pause durations, it is likely that different classes of receptors are involved in the arrest and pause processes as found in previous work on monocyte-endothelial binding under flow (Kukreti et al., 1997).

It is also possible that different receptors may be involved at different levels of shear stress because higher k_{off}^{o} values

were obtained at shear stresses below 1 dyn/cm^2 (Fig. 8). Below this shear stress, α_4 and β_2 integrins may be stronger mediators of cell adhesion than selectins, which dominate at higher shear stresses (Konstantopoulos et al., 1998). Mono Mac 6 cells have been found to be similar to human blood monocytes in adhesion properties with binding to HUVECs occurring via ICAM-1, VCAM-1, and E-selectin (Erl et al., 1995). Human blood monocytes express several adhesion molecules that may be involved in adhesion to endothelial cells, including LFA-1 and MAC-1, which bind to ICAM-1; VLA-4, which binds to VCAM-1; L-selectin; and sialyl-Lewis x, which binds to E- and P-selectins (Prieto et al., 1994).

We examined whether the presence of high-molecular-weight dextran might affect adhesion, possibly by sterically blocking binding in solution or by becoming entangled with microvilli. Preincubation of HUVECs with dextran solutions before introduction of Mono Mac 6 cells in the absence of dextran did not significantly affect the rolling velocity. Furthermore, rolling was less and tethering greater in the high-viscosity dextran solutions than in the media alone. This result is the opposite of what would occur if dextran were blocking adhesion.

The mechanism by which increased force leads to increased bond formation is unknown; however, there are several possibilities. The increased force with which monocytes contact the endothelium could cause the monocyte and its microvilli to deform to a greater extent, thereby creating greater contact area for adhesion as shown for leukocytes in vivo and in side-view flow chambers (Cao et al., 1998; House and Lipowsky, 1988). Leukocyte contact area on a surface can increase as much as twofold as shear stress is increased to 20 dyn/cm^2 (Dong and Lei, 2000). However, gross leukocyte deformation was not appreciable at 2.9 dyn/cm^2 (Dong and Lei, 2000), corresponding to 7.3-cP media at 40 s^{-1}. This shear stress resulted in a significant decrease in rolling velocities from 42 $\pm$ 3.7 to 31 $\pm$ 1.4 μm/s. There may be compression of microvilli that does not translate into deformation of the entire cell.

Alternatively, higher forces may be sufficient to increase the probability that the cell penetrates steric or repulsive barriers. The source of this barrier is the glycocalyx, an outer layer of glycoproteins with a net negative charge on the cell's surface. Although endothelial glycocalyx formation is most likely significantly less in vitro than in vivo, there are still electrostatic and steric boundaries to overcome. Gycocalyx thickness ranges from 45 to 81 nm in rabbit arteries (Haldenby et al., 1994), whereas adhesion receptors are significantly shorter: ICAM-1 is ~18.7 nm long; VCAM-1, 25 nm; E-selectin, 28 nm; and P-selectin, 40 nm (Springer, 1990). L-selectin on monocytes, however, binds to surface heparan sulfate proteoglycans on aortic endothelium (Giuffrè et al., 1997; Koenig et al., 1998). Glycocalyx fibers are displaced by adhesion events, possibly illustrating that glycocalyx rearrangement must occur to allow adhesion receptors to bind (Soler et al., 1998). Fetal calf aortic endothelial cells cultivated in vitro were found to have a surface charge due predominantly to sialic acid followed by chondroitin sulfate and heparan sulfate (Van Damme et al., 1994). Different mechanisms may dominate for tethering as compared with rolling cells under shear flow (Finger et al., 1996). The increase in tethering frequencies with shear stress at constant shear rate may be due to more frequent penetration of steric or charge barriers, whereas the decrease in rolling velocity and increase in arrest durations may be due to the greater contact area and thereby greater propensity for multiple bond formation.

In summary, these studies indicate that leukocyte rolling and arrest on endothelium are influenced by both the contact time and force. As shear rate is increased, the rolling velocity increases, the tethering frequency drops, and the arrest durations decrease. The applied force on a cell increases the fraction of initial adhesive events, the stability of rolling, and the duration of arrest events. Such stable adhesions may help explain how monocytes can adhere to arterial endothelium during atherosclerosis and the preponderance of plaque formation with conditions such as hyperviscosity syndrome (Dobberstein et al., 1999).

A subculture of Mono Mac 6 cells was generously provided by Dr. H. W. L. Ziegler-Heitbrock (Universitat Munchen).
This work was supported by National Institutes of Health grant HL-57446. Flow cytometry was performed at the Cancer Center Flow Cytometry Shared Resource, Duke University.

REFERENCES

Alon, R., S. Chen, K. D. Puri, E. B. Finger, and T. A. Springer. 1997. The kinetics of L-selectin tethers and the mechanics of selectin-mediated rolling. *J. Cell Biol.* 138:1169–1180.

Alon, R., D. A. Hammer, and T. A. Springer. 1995. Lifetime of the P-selectin-carbohydrate bond and its response to tensile force in hydrodynamic flow. *Nature.* 374:539–542.

Baldwin, A. L., N. Z. Wu, and D. L. Stein. 1991. Endothelial surface charge of intestinal mucosal capillaries and its modulation by dextran. *Microvasc. Res.* 42:160–178.

Barber, K. 1997. Effects of shear and recirculating flow on U937 cell adhesion to activated endothelium: implications in atherosclerosis. Ph.D. thesis. Duke University, Durham, NC. 322 pp.

Bates, D. M., and D. G. Watts. 1988. Nonlinear Regression Analysis and Its Applications. John Wiley and Sons, New York.

Beekhuizen, H., and R. van Furth. 1993. Monocyte adherence to human vascular endothelium. *J. Leukocyte Biol.* 54:363–378.

Bell, G. I. 1978. Models for the specific adhesion of cells to cells. *Science.* 200:618–627.

Bruehl., R. E., T. A. Springer, and D. F. Bainton. 1996. Quantitation of L-selectin distribution on human leukocyte microvilli by immunogold labeling and electron microscopy. *J. Histochem. Cytochem.* 44:835–844.

Cao, J., B. Donell, D. R. Deaver, M. B. Lawrence, and C. Dong. 1998. In vitro side-view imaging technique and analysis of human T-leukemic cell adhesion to ICAM-1 in shear flow. *Microvasc. Res.* 55:124–137.

Chang, K.-C., and D. Hammer. 1999. The forward rate of binding of surface-tethered reactants: effect of relative motion between two surfaces. *Biophys. J.* 76:1280–1292.

Chen, S., and T. Springer. 1999. An automatic braking system that stabilizes leukocyte rolling by an increase in selectin bond number with shear. *J. Cell Biol.* 144:185–200.

Chesla, S., P. Selvaraj, and C. Zhu. 1998. Measuring two-dimensional receptor-ligand binding kinetics by micropipette. *Biophys. J.* 75: 1553–1572.

Cozens-Roberts, C., J. A. Quinn, and D. A. Lauffenburger. 1990. Receptor-mediated adhesion phenomena: model studies with the radial-flow detachment assay. *Biophys. J.* 58:107–125.

Dobberstein, H., U. Solbach, A. Weinberger, and S. Wolf. 1999. Correlation between retinal microcirculation and blood viscosity in patients with hyperviscosity syndrome. *Clin. Hemorheol. Microcirc.* 20:31–35.

Dong, C., and X. X. Lei. 2000. Biomechanics of cell rolling: shear flow, cell-surface adhesion, and cell deformability. *J. Biomech.* 33:35–43.

Erl, W., C. Weber, C. Wardemann, and P. C. Weber. 1995. Adhesion properties of Mono Mac 6, a monocytic cell line with characteristics of mature human monocytes. *Atherosclerosis.* 113:99–107.

Finger, E. B., R. E. Bruehl, D. F. Bainton, and T. A. Springer. 1996. A differential role for cell shape in neutrophil tethering and rolling on endothelial selectins under flow. *J. Immunol.* 157:5085–5096.

Giuffrè, L., A.-S. Cordey, N. Monai, Y. Monai, Y. Tardy, M. Schapira, and O. Spertini. 1997. Monocyte adhesion to activated aortic endothelium: role of L-selectin and heparan sulfate proteoglycans. *J. Cell Biol.* 136: 945–956.

Goldman, A. J., R. G. Cox, and H. Brenner. 1967. Slow viscous motion of a sphere parallel to a plane wall. II. Couette flow. *Chem. Eng. Sci.* 22:653–660.

Haldenby, K. A., D. C. Chappell, C. P. Winlove, K. H. Parker, and J. A. Firth. 1994. Focal and regional variations in the composition of the glycocalyx of large vessel endothelium. *J. Vasc. Res.* 31:2–9.

Hammer, D. A., and S. M. Apte. 1992. Simulation of cell rolling and adhesion on surfaces in shear flow: general results and analysis of selectin-mediated neutrophil adhesion. *Biophys. J.* 63:35–57.

House, S. D., and H. H. Lipowsky. 1988. In vivo determination of the force of leukocyte-endothelium adhesion in the mesenteric microvasculature of the cat. *Circ. Res.* 63:658–668.

Kaplanski, G., C. Farnarier, O. Tissot, A. Pierres, A. M. Benoliel, M. C. Alessi, S. Kaplanski, and P. Bongrand. 1993. Granulocyte-endothelium initial adhesion: analysis of transient binding events mediated by E-selectin in a laminar shear flow. *Biophys. J.* 64:1922–1933.

Koenig, A., K. Norgard-Sumnicht, R. Linhardt, and A. Varki. 1998. Differential interactions of heparin and heparan sulfate glycosaminoglycans with the selectins. *J. Clin. Invest.* 101:877–889.

Konstantopoulos, K., S. Kukreti, and L. V. McIntire. 1998. Biomechanics of cell interactions in shear fields. *Adv. Drug Delivery Rev.* 33:141–164.

Kukreti, S., L. Konstantopoulos, C. W. Smith, and L. V. McIntire. 1997. Molecular mechanisms of monocyte adhesion to interleukin-1β-stimulated endothelial cells under physiologic flow conditions. *Blood.* 89:4104–4111.

Lawrence, M. B., G. S. Kansas, E. J. Kunkel, and K. Ley. 1997. Threshold levels of fluid shear promote leukocyte adhesion through selectins (CD62L, P, E). *J. Cell Biol.* 136:717–727.

Munn, L. L., R. J. Melder, and R. K. Jain. 1994. Analysis of cell flux in the parallel plate flow chamber: implications for cell capture studies. *Biophys. J.* 67:889–895.

Prieto, J., A. Eklund, and M. Patarroyo. 1994. Regulated expression of integrins and other adhesion molecules during differentiation of monocytes into macrophages. *Cell. Immunol.* 156:191–211.

Reinhardt, P. H., and P. Kubes. 1998. Differential leukocyte recruitment from whole blood via endothelial adhesion molecules under shear conditions. *Blood.* 92:4691–4699.

Schmidtke, D. W., and S. L. Diamond. 2000. Direct observation of membrane tethers formed during neutrophil attachment to platelets or P-selectin under physiological flow. *J. Cell Biol.* 149:719–729.

Shao, J.-Y., H. P. Ting-Beall, and R. Hochmuth. 1998. Static and dynamic lengths of neutrophil microvilli. *Proc. Natl. Acad. Sci. U.S.A.* 95: 6797–6802.

Smith, M. J., E. L. Berg, and M. B. Lawrence. 1999. A direct comparison of selectin-mediated transient, adhesive events using high temporal resolution. *Biophys. J.* 77:3371–3383.

Soler, M., S. Desplat-Jego, B. Vacher, L. Ponsonnet, M. Fraterno, P. Bongrand, J.-M. Martin, and C. Foa. 1998. Adhesion-related glycocalyx study: quantitative approach with imaging-spectrum in the energy filtering transmission electron microscope (EFTEM). *FEBS.* 429:89–94.

Springer, T. A. 1990. Adhesion receptors of the immune system. *Nature.* 346:425–434.

Swift, D. G., R. G. Posner, and D. A. Hammer. 1998. Kinetics of adhesion of IgE-sensitized rat basophilic leukemia cells to surface-immobilized antigen in couette flow. *Biophys. J.* 75:2597–2611.

Takahashi, M., U. Ikeda, J.-I. Masuyama, S.-I. Kitagawa, T. Kasahara, M. Saito, S. Kano, and K. Shimada. 1994. Involvement of adhesion molecules in human monocyte adhesion to and transmigration through endothelial cells in vitro. *Atherosclerosis.* 108:73–81.

Taylor, A. D., S. Neelamegham, J. D. Hellums, C. W. Smith, and S. I. Simon. 1996. Molecular dynamics of the transition from L-selectin- to β_2-integrin-dependent neutrophil adhesion under defined hydrodynamic shear. *Biophys. J.* 71:3488–3500.

Van Damme, M.-P. I., J. Tiglias, N. Nemat, and B. N. Preston. 1994. Determination of the charge content at the surface of cells using a colloid titration technique. *Anal. Biochem.* 223:62–70.

von Andrian, U. H., S. R. Hasslen, R. D. Nelson, S. L. Erlandsen, and E. C. Butcher. 1995. A central role for microvillous receptor presentation in leukocyte adhesion under flow. *Cell.* 82:989–999.

Watanabe, T., and J. Fan. 1998. Atherosclerosis and inflammation: mononuclear cell recruitment and adhesion molecules with reference to the implication of ICAM-1/LFA-1 pathway in atherogenesis. *Int. J. Cardiol.* 66:S45–S53.

Zhao, Y., S. Chien, and R. Skalak. 1995. A stochastic model of leukocyte rolling. *Biophys. J.* 69:1309–1320.

Zhu, C. 2000. Kinetics and mechanics of cell adhesion. *J. Biomech.* 33:23–33.